TECHNICAL UNIVERSITY OF CLUJ-NAPOCA

ACTA TECHNICA NAPOCENSIS

Series: Applied Mathematics, Mechanics, and Engineering
Vol. 69, Issue Special II, May, 2026

UNCERTAINTY EVALUATION ON LINEWIDTH MEASUREMENT USING AN OPTICAL MICROSCOPIC SYSTEM CALIBRATED BY BOTH A LASER INTERFEROMETER AND A LINEWIDTH STANDARD

Chu-Shik KANG, Jae Yong LEE, Sunghoon EOM, Jong-Ahn KIM and Jae Heun WOO

Abstract: *An optical microscopic system for precise linewidth measurement has been developed. The system is capable of measuring linewidths that are either narrower or wider than the microscope's field of view, and can be applied to both transparent and opaque lines. It is calibrated using a laser interferometer and a linewidth standard, the latter calibrated by a foreign National Metrology Institute. This paper presents the measurement system and provides a detailed evaluation of the measurement uncertainty.*

Key words: *Linewidth, optical microscopy, calibration, measurement uncertainty.*

1. INTRODUCTION

In modern industry, linewidth is a critical physical parameter that significantly influences the performance, reliability, and manufacturing yield of products, particularly in sectors such as semiconductors, flat panel displays, micro electro-mechanical systems (MEMS), opto-electronics, and precision manufacturing. Various techniques have been developed to measure linewidths with high accuracy, including optical microscopy, critical dimension scanning electron microscopy (CD-SEM) and atomic force microscopy (AFM) [1]-[3].

The Korea Research Institute of Standards and Science (KRISS) has recently developed a linewidth measurement system based on optical microscopy, capable of measuring linewidths in the range of 1 μm to 2000 μm. In this system, the unit pixel size of the optical microscope image is calibrated using a laser interferometer to ensure dimensional accuracy. Additionally, a certified reference linewidth standard is utilized to determine the threshold level of the image intensity profile, which plays a critical role in the definition of the linewidth. Consequently, the measured linewidths achieve metrological traceability to the SI unit of length, the meter, not only through the wavelength of the laser used in the interferometric calibration of the pixel size, but also via the certified value of the reference linewidth standard used in determining the threshold intensity level.

This paper provides a brief overview of the developed measurement system and presents a detailed evaluation of measurement uncertainty for the specific case in which the system is calibrated using both the laser wavelength and a reference linewidth standard.

2. THE MEASUREMENT SYSTEM

2.1 Structure of the measurement system

The developed measurement system is based on optical microscopy. The main components of the system include an optical microscope, a motorized translating sample stage, a laser interferometer, a CMOS camera, a slit and a photo-multiplier tube, measurement software, a field programmable gate array, and a personal computer. Figure 1 shows the schematic diagram of the system.

The system is designed to measure widths of both clear and opaque lines, and provides two measurement modes, which are full-field camera

mode (FFCM) and confocal slit scanning mode (CSSM).

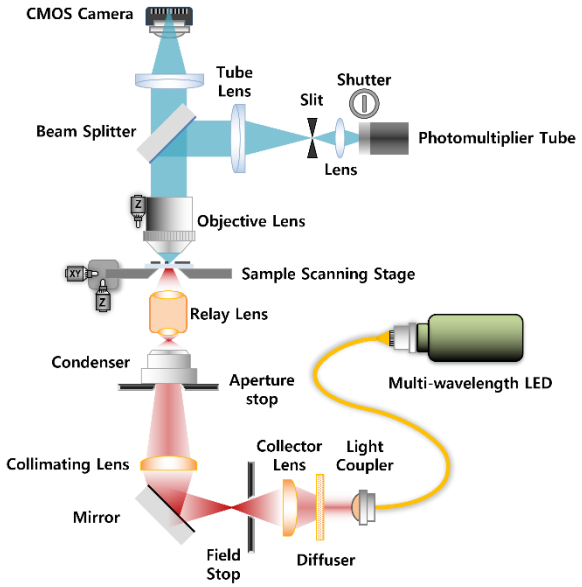


Fig. 1 Schematic diagram of the measurement system

In FFCM, the intensity profile of a line is directly obtained from the image captured by a CMOS camera, whereas in CSSM, it is obtained from the signal of a photomultiplier tube which detects the light passing through a slit while the sample is scanned by the moving stage.

Usually, FFCM is used for measuring lines narrower than the field of view (FOV) of the microscope, and CSSM for those wider than the FOV. However, the FFCM can also be used to measure lines wider than the FOV by scanning the stage, combining the information from the images including each edge, and the laser interferometer. In all measuring modes, a common algorithm is used to determine the linewidth value.

This paper will focus on linewidth measurements by using FFCM. The optical microscope is equipped with two objective lenses. The lens with magnification of 10× (numerical aperture (NA): 0.3) is used for measurement of linewidths greater than 40 μm, and the other one having magnification of 40× (NA: 0.75) for measuring linewidths of 40 μm and less, down to 1 μm. To reduce the effect of magnification variation across the FOV, the line under measurement was always placed at the center of the FOV, which was implemented automatically by simply selecting the target line from the image with the mouse. To minimize measurement errors that occur due to deviation from optimal focusing conditions, a focus monitoring function is used which enables us to make measurements when the slope of the edge profile is maximized, resulting in excellent measurement repeatability. A threshold level for the intensity profile of the line image must be defined to enable accurate determination of the line width. The threshold was calibrated using a linewidth standard, ensuring that the measured linewidth of the standard matches its certified value. Separate threshold levels for opaque and transparent lines were established at each magnification. More detailed information about this system is to be found elsewhere [4]

2.2 Measurement principle

A concise summary of the measurement principle underlying the FFCM is as follows: An image of the target line is acquired using a CMOS camera. The linewidth is determined from the corresponding intensity profile as the distance between the two points at which the profile intersects a predefined threshold level (see Fig. 2). Since the horizontal axis of the intensity profile is expressed in pixels, this distance is initially obtained as a number of pixels. The physical linewidth is then obtained by applying a conversion factor, which corresponds to the pixel size in physical units

2.3 Calibration of the measurement system

2.3.1 Calibration of the pixel size

Prior to the linewidth measurements, the pixel size was calibrated using a linewidth standard and a laser interferometer. The target line was first located at the left side of the FOV. The x-axis data are linearly interpolated so that the distance between neighboring points is nominally around 20 nm. From the interpolated intensity profile, the pixel coordinate of the line center was measured. Then the sample stage was translated so that the line is located at the right side of the FOV.

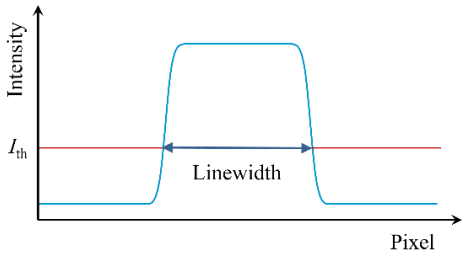


Fig. 2 Determination of the linewidth from an intensity profile of a microscope image using a threshold intensity level, I_{th}.

During the stage translation, the displacement was measured by a laser interferometer whose nonlinearity was compensated using the technique of fitting an ellipse to the dual quadrature signals of the interferometer [5]. Again, the pixel coordinate of the line center was measured from the interpolated intensity profile. The pixel size was determined by comparing the difference in pixel counts between two positions to the corresponding displacement of the stage.

2.3.2 Calibration of the threshold level

Linewidth standards, produced and calibrated by the National Physical Laboratory (NPL) of the United Kingdom, were employed as the reference for threshold level calibration. The calibration begins by selecting a target line using the mouse interface, which automatically centers the selected line within the FOV, followed by image acquisition. The captured image is processed to obtain an interpolated intensity profile to enhance resolution. Tentative edge positions are initially determined using a temporary threshold level, defined as 50 % of the difference between the maximum and minimum intensity values of the profile. To estimate the minimum intensity level accurately, two baseline regions, one on each side of the line, are selected. The intensity data within these regions are together fitted to a straight line, and the resulting slope is subtracted from the entire profile to flatten the baseline. The average intensity over the two baseline regions is then taken as the lower intensity level $I_{\text{ref, low}}$. Next, a central region from the area containing the line is selected, and the upper intensity level $I_{\text{ref, up}}$ is computed as the average intensity within this region. The threshold intensity level, I_{th}, is defined as $T_c \Delta I$, where ΔI denotes the difference between $I_{\text{ref, up}}$ and $I_{\text{ref, low}}$, and T_c is a threshold ratio, whose value is between zero and one. I_{th} is tunable by varying T_c. For each threshold level, a linear fit is applied to seven data points on each edge near the threshold level. The distance between the two points where the fitted lines intersect the threshold level is obtained in terms of number of pixels. The conversion factor, F_c, which corresponds to the calibrated pixel size, is multiplied to this number of pixels to obtain the physical linewidth value. This procedure was applied to multiple linewidth standards to determine the optimal threshold ratio that minimizes the sum of squared deviations between the measured and certified values. This procedure was performed separately for each of the two magnification settings.

3. UNCERTAINTY EVALUATION OF LINEWIDTH MEASUREMENT

Uncertainty of linewidth measured by the developed system is evaluated according to the ISO/IEC 98-3 [6].

3.1 Measurement function

Let the linewidth be denoted as W_L. The measurement function for W_L is a function of the two (left and right) pixel positions, P_l and P_r, at which the image intensity profile intersects the threshold intensity level, I_{th}, on the left and right edges, respectively, and of the conversion factor, F_c, which corresponds to the calibrated pixel length. If l_t, δl_r, δl_f and δl_c represent the correction terms for thermal effect, random effect, focus effect, and cosine error, respectively, the measurement function is expressed as Eq. (1).

$$W_L = F_c\left(P_r - P_l\right) + l_t + \delta l_r + \delta l_f + \delta l_c \qquad (1)$$

As explained earlier, the conversion factor F_c is determined by dividing the stage displacement L measured by a laser interferometer, by ΔP, the difference between the two pixel positions: P_s, the center pixel

when the line under measurement is positioned on the left side of the FOV, and P_e, the center pixel after the line has been moved to the right side of the FOV by the translation stage. Therefore, F_c can be expressed as shown in Eq. (2).

$$F_c = \frac{L}{\Delta P} = \frac{L}{P_e - P_s} \tag{2}$$

Let a_1 and b_1 denote the slope and intercept of the line fitted to the intensity data near the threshold at the left edge, and let a_2 and b_2 denote those at the right edge. Then, the positions P_l and P_r are determined by evaluating the inverse of each fitted line at the threshold level, and are expressed as

$$P_l = \frac{I_{th} - b_1}{a_1} = \frac{T_c \Delta I - b_1}{a_1},\ P_r = \frac{T_c \Delta I - b_2}{a_2}, \tag{3}$$

where ΔI denotes the difference of upper and lower intensity levels, and T_c is the threshold intensity ratio, ranging between 0 and 1. Thus, the measurement function can be finally expressed as Eq. (4).

$$W_L = \frac{L}{\Delta P}\left(\frac{T_c \Delta I - b_2}{a_2} - \frac{T_c \Delta I - b_1}{a_1}\right) + l_t + \delta l_r + \delta l_f + \delta l_c \tag{4}$$

3.2 Combined standard uncertainty equation

By applying the law of propagation of uncertainty to the measurement function, the equation for the combined standard uncertainty is obtained as Eq. (5).

$$\begin{aligned} u_c^2 = {} & c_L^2 u^2(L) + c_{\Delta P}^2 u^2(\Delta P) + c_{T_c}^2 u^2(T_c) \\ & + c_{\Delta I}^2 u^2(\Delta I) + c_{a_1}^2 u^2(a_1) + c_{b_1}^2 u^2(b_1) \\ & + c_{a_2}^2 u^2(a_2) + c_{b_2}^2 u^2(b_2) + c_{l_t}^2 u^2(l_t) \\ & + c_{\delta l_r}^2 u^2(\delta l_r) + c_{\delta l_f}^2 u^2(\delta l_f) + c_{\delta l_c}^2 u^2(\delta l_c) \\ & + 2c_{a_1} c_{b_1} u(a_1, b_1) + 2c_{a_2} c_{b_2} u(a_2, b_2) \end{aligned} \tag{5}$$

Sensitivity coefficient c_i for each input quantity x_i is as follows.

$$c_L = \frac{1}{\Delta P}\left(\frac{T_c \Delta I - b_2}{a_2} - \frac{T_c \Delta I - b_1}{a_1}\right) \square \frac{W_L}{L} \tag{6}$$

$$c_{\Delta P} = \frac{-L}{\Delta P^2}\left(\frac{T_c \Delta I - b_2}{a_2} - \frac{T_c \Delta I - b_1}{a_1}\right) \square \frac{W_L}{\Delta P} \tag{7}$$

$$c_{T_c} = \frac{L \Delta I}{\Delta P}\left(\frac{1}{a_2} - \frac{1}{a_1}\right) \tag{8}$$

$$c_{\Delta I} = \frac{L T_c}{\Delta P}\left(\frac{1}{a_2} - \frac{1}{a_1}\right) \tag{9}$$

$$c_{a_1} = \frac{L}{\Delta P}\left(\frac{T_c \Delta I - b_1}{a_1^2}\right) \tag{10}$$

$$c_{b_1} = \frac{L}{a_1 \Delta P} \tag{11}$$

$$c_{a_2} = \frac{-L}{\Delta P}\left(\frac{T_c \Delta I - b_2}{a_2^2}\right) \tag{12}$$

$$c_{b_2} = \frac{-L}{a_2 \Delta P} \tag{13}$$

$$c_{l_t} = c_{\delta l_r} = c_{\delta l_f} = c_{\delta l_c} = 1 \tag{14}$$

3.3 Evaluation of standard uncertainties

3.3.1 $u(L)$

Standard uncertainty of the displacement measurement by a laser interferometer during the pixel size calibration can be evaluated by Eq. (15),

$$\begin{aligned} u(L)^2 = {} & u(L_r)^2 + u(L_\lambda)^2 + u(L_n)^2 \\ & + u(L_c)^2 + u(L_{Ab})^2 + u(L_{nl})^2 \end{aligned} \tag{15}$$

where the uncertainty components in the right side of the equation are attributed to repeatability, vacuum wavelength of the laser, refractive index of air, cosine error, Abbe error, and nonlinearity of the interferometer, respectively.

Uncertainty due to random effect is evaluated by the standard deviation of the mean:

$$u(L_r) = s_L / \sqrt{n_L} \tag{16}$$

where s_L and n_L denote the experimental standard deviation, and the number of repeated measurements, respectively.

Uncertainty due to the vacuum wavelength of the laser is evaluated as Eq. (17),

$$u(L_\lambda)^2 = L^2\left[\{U_r(\lambda)/k\}^2 + u_r(\lambda_{lts})^2\right] \tag{17}$$

where $U_r(\lambda)$ and k denote the relative expanded uncertainty and coverage factor reported in the calibration certificate, and $u_r(\lambda_{lts})$ is the relative long-term stability of the vacuum wavelength provided by the laser manufacturer.

Uncertainty due to the refractive index of air is evaluated as Eq. (18),

$$u(L_n) = L \cdot u(n) \tag{18}$$

where n denotes the refractive index of air. In linewidth measurements, the refractive index of air was not measured but instead assumed to be the value under standard atmospheric conditions. The range in which the temperature, relative humidity, atmospheric pressure, and carbon dioxide concentration of the actual measurement environment may deviate from the standard conditions was estimated, and the uncertainty of the refractive index of air was evaluated based on an empirical equation [7] .

If the optical axis of the laser is not aligned with the travel axis of the stage, a cosine error may occur. Assuming that the misalignment angle between the two axes is within θ_c , the associated uncertainty is given by Eq. (19).

$$u(L_c) = L\theta_c^2 / \sqrt{48} \tag{19}$$

The uncertainty due to the Abbe error is evaluated from a rectangular probability distribution with the maximum value of the Abbe error as the half-width, as expressed in Eq. (20), where L_A denotes the offset between the specimen surface and the optical axis of the laser, and θ_A is the maximum angular motion error of the stage.

$$u(L_{Ab}) = L_A\theta_A / \sqrt{3} \tag{20}$$

The uncertainty due to the nonlinearity, L_{nl}, of the laser interferometer, is obtained from a rectangular probability distribution whose half-width is equal to L_{nl}.

$$u(L_{nl}) = L_{nl} / \sqrt{3} \tag{21}$$

3.3.2 $u(\Delta P)$

ΔP represents the number of pixels between the central coordinates of the line on the screen as it moves from the left to the right side of the FOV. Its standard uncertainty consists of two components: the uncertainty due to random effect and the uncertainty due to finite resolution.

$$u^2(\Delta P) = u^2(\Delta P_{ran}) + u^2(\Delta P_{res}) \tag{22}$$

The first component is evaluated as $s_{\Delta P} / \sqrt{n_{\Delta P}}$, where $s_{\Delta P}$ and $n_{\Delta P}$ denote the experimental standard deviation, and the number of repeated measurements, respectively. The second uncertainty component is evaluated based on Eq. (23) (See Fig. 3).

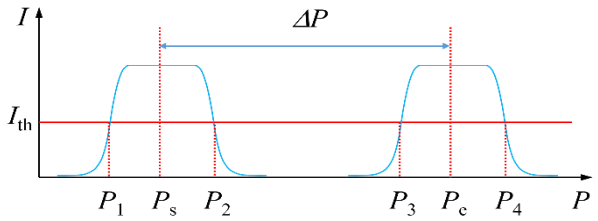


Fig. 3 Definition of *ΔP*.

$$\begin{aligned} \Delta P &= P_e - P_s \\ &= (P_3 + P_4)/2 - (P_1 + P_2)/2 \end{aligned} \tag{23}$$

Applying the law of propagation of uncertainty to this equation gives the result:

$$u(\Delta P_{res}) = R / (2\sqrt{3}) \tag{24}$$

where, R represents the resolution of the pixel-based coordinate system. When a N-point interpolation was used, R equals to $1/N$.

3.3.3 $u(T_c)$

The threshold ratio, T_c , determined while measuring the linewidth standards of NPL, is the ratio of the threshold intensity to the difference between the upper and lower intensity levels ($T_c = I_{th,ref} / \Delta I_{ref}$). As described in section 2.3.2, T_c was determined based on various linewidth standards such that the chi-square value was minimized. Taking into account the uncertainty of this process, the measurement function for T_c is given by Eq. (25).

$$T_c = \frac{I_{th,ref}}{\Delta I_{ref}} + \delta T_c \tag{25}$$

The last term in the equation is a correction term for the fitting error introduced during the T_c determination process, and its expected value is zero. Thus $u(T_c)$ becomes:

$$u^2(T_c) = \frac{u^2(I_{th,ref})}{\Delta I_{ref}^{\ 2}} + \left(\frac{-I_{th,ref}}{\Delta I_{ref}^{\ 2}}\right)^2 u(\Delta I_{ref})^2 + u^2(\delta T_c) \quad (26)$$

The first component $u(I_{th,ref})$ is the uncertainty of the threshold intensity. It consists of two uncertainty components.

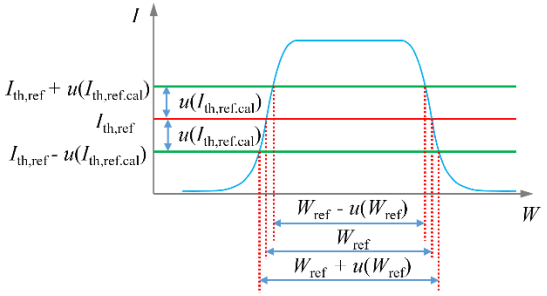


Fig. 4 Evaluation of $u(I_{th,ref})$ using the standard uncertainty of the linewidth standard

$$u(I_{th,ref}) = \sqrt{u^2(I_{th,ref,cal}) + u^2(I_{th,ref,dev})} \quad (27)$$

The first component $u(I_{th,ref,cal})$ is the uncertainty due to the uncertainty of the certified value of the linewidth standard. Let the expanded uncertainty and coverage factor of the certified value be denoted by U_{ref} and k_{ref}, respectively. As can be seen in Fig. 4, $u(I_{th,ref,cal})$ can be obtained as

$$u(I_{th,ref,cal}) = \frac{S_{edge} u(W_{ref})}{2} = \frac{S_{edge} U_{ref}}{2k_{ref}}, \quad (28)$$

where S_{edge} and $u(W_{ref})$ refer to the slope (in μm^{-1}) at the edge of the linewidth profile corresponding to the threshold intensity, and the standard uncertainty of the reference linewidth, respectively, and U_{ref} and k_{ref} denote the expanded uncertainty and the coverage factor stated in the calibration certificate of the linewidth standards.

Even though T_c was optimized to minimize the chi-square, its use will result in slight deviation of the measured values from the certified values of the linewidth standards. The effect of this residual is taken as the second component of Eq. (27).

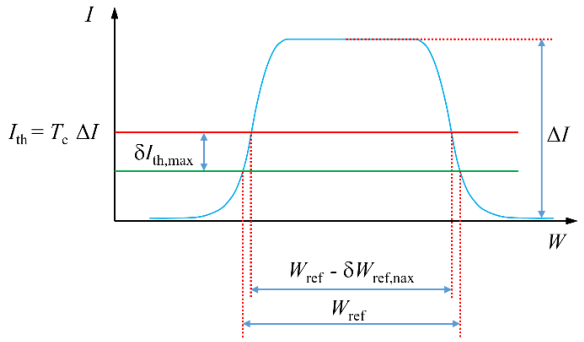


Fig. 5 Diagram showing how to evaluate $u(I_{th,ref,dev})$.

This uncertainty can be calculated from a rectangular distribution, with $\delta I_{th,max}$ (the intensity deviation corresponding to the maximum deviation $\delta W_{ref,max}$ between the measured and certified values of the 13 linewidth standards) as the half-width, as shown in Eq. (29) (See Fig. 5).

$$u(I_{th,ref,dev}) = \frac{S_{edge} \delta W_{ref,max})}{2\sqrt{3}} \quad (29)$$

The second component of $u(T_c)$ is $u(\Delta I_{ref})$. As ΔI_{ref} is equal to the difference of upper and lower intensity levels, $I_{ref,up} - I_{ref,down}$, $u(\Delta I_{ref})$ becomes

$$u(\Delta I_{ref}) = \sqrt{u^2(I_{ref,up}) + u^2(I_{ref,down})} = \sqrt{\left(\frac{s_{ref,up}}{\sqrt{n_{ref,up}}}\right)^2 + \left(\frac{s_{ref,down}}{\sqrt{n_{ref,down}}}\right)^2} \quad (30)$$

where $s_{ref,up}$ and $s_{ref,down}$ denote the standard deviations of the intensity data at the upper and lower intensity levels, respectively, while $n_{ref,up}$ and $n_{ref,down}$ represent the corresponding numbers of data points.

The last component of $u(T_c)$ is $u(\delta T_c)$, which accounts for the uncertainty associated with the optimization process for determining T_c. FigureFig. 6 shows thee chi-square values of the 13 linewidth standards measured with 13 different T_c values, calculated by Eq. (31).

$$\chi^2(T_{c,i}) = \sum_{j=1}^{N} \frac{\{W_j(T_{c,i}) - W_{j,ref}\}^2}{\sigma_j^{\ 2}} \quad (31)$$

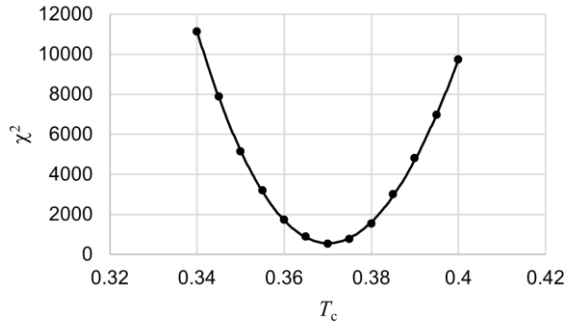


Fig. 6 Chi-square values for various T_c values.

The uncertainty $u(\delta T_c)$ arising from the optimization process is evaluated as the change in T_c associated with an increase of 1 in the chi-square value from its minimum.

3.3.4 $u(\Delta I)$

This is the uncertainty of ΔI, the difference between the upper and lower intensity levels used to determine the threshold intensity in the intensity profile of the linewidth under measurement. This term is evaluated in the same way as $u(\Delta I_{\text{ref}})$.

$$u(\Delta I) = \sqrt{u^2(I_{\text{up}}) + u^2(I_{\text{down}})} = \sqrt{\left(\frac{s_{\text{up}}}{\sqrt{n_{\text{up}}}}\right)^2 + \left(\frac{s_{\text{down}}}{\sqrt{n_{\text{down}}}}\right)^2} \quad (32)$$

where s_{up} and s_{down} denote the standard deviations of the intensity data at the upper and lower intensity levels, respectively, while n_{up} and n_{down} represent the corresponding numbers of data points.

3.3.5 $u(a_1)$ and $u(a_2)$

The standard uncertainty associated with the slope of each fitted line is derived from the least-squares fitting process.

$$u(a_i) = s_i\sqrt{\frac{n_i}{D_i}} \qquad (i = 1, 2) \quad (33)$$

where i equals 1 for the left edge and 2 for the right edge, n_i denotes the number of data used for the fitting, and s_i, D are as follows.

$$s_i = \sqrt{\frac{1}{n_i - 2}\sum_{k=1}^{n_i}\left\{I_{i,k} - \left(a_i I_{i,k} + b_i\right)\right\}^2} \quad (34)$$

$$D_i = n_i\sum_{k=1}^{n_i} I_{i,k}^2 - \left(\sum_{k=1}^{n_i} I_{i,k}\right)^2 \quad (35)$$

3.3.6 $u(b_1)$ and $u(b_2)$

The standard uncertainty associated with the intercept of each fitted line is also derived from the least-squares fitting process.

$$u(b_i) = s_i\sqrt{\frac{1}{D_i}\sum_{k=1}^{n_i} I_{i,k}^2} \qquad (i = 1, 2) \quad (36)$$

3.3.7 $u(a_1, b_1)$ and $u(a_2, b_2)$

The covariance between the slope and intercept of the fitted line is obtained during the fitting process using Eq. (37).

$$u(a_i, b_i) = u(a_i)u(b_i)\frac{\sum_{k=1}^{n_i} I_{i,k}}{\sqrt{n_i\sum_{k=1}^{n_i} I_{i,k}^2}} \quad (37)$$

3.3.8 $u(l_t)$

The term l_t represents the correction term for thermal effect. If the coefficient of thermal expansion of the linewidth standard is α, and the temperature at the time of measurement is t, l_t is expressed as:

$$l_t = -\alpha(t - 20°\text{C})W_L \quad (38)$$

Thus, $u(l_t)$ can be express as Eq. (**39**).

$$u^2(l_t) = \{-(t - 20°\text{C})W_L\}^2 u^2(\alpha) + (-\alpha W_L)^2 u^2(t) \quad (39)$$

Since the measurement length is very short, uncertainty contribution by thermal effect is negligible.

3.3.9 $u(\delta l_r)$

This term represents the standard uncertainty arising from random effects, corresponding to the standard deviation of the mean calculated from n repeated measurements of the linewidth.

$$u(\delta l_r) = s/\sqrt{n} \quad (40)$$

where s denotes the standard deviation.

3.3.10 $u(\delta l_f)$

This term is the uncertainty caused by defocusing of the microscope from its optimal focal position. If the focus is assumed to always remain within a deviation of $\pm\delta f$ from the optimal position, the standard uncertainty can be expressed as follows.

$$u(\delta l_{\mathrm{f}}) = \frac{\partial W_{\mathrm{L}}}{\partial f} u(f) = \frac{\partial W_{\mathrm{L}}}{\partial f} \frac{\delta f}{\sqrt{3}} \tag{41}$$

The sensitivity coefficient $\partial W_{\mathrm{L}} / \partial f$ is experimentally obtained by systematically varying the focusing condition and analyzing the resulting changes in the measured values.

3.3.11 $u(\delta l_{\mathrm{c}})$

This term represents the standard uncertainty component of the linewidth due to the cosine error caused by the misalignment of the linewidth specimen. If the line direction of the linewidth specimen deviates from the y-axis on the image by an angle within $\pm\theta$, then $u(\delta l_{\mathrm{c}})$ can be evaluated as Eq. (42).

$$u(\delta l_{\mathrm{c}}) = \theta^2 W_{\mathrm{L}} / \sqrt{45} \tag{42}$$

3.3 Combined standard uncertainty

Using the sensitivity coefficients calculated by Eq. (6)-(14), and the standard uncertainties evaluated by Eq. (15)-(42), the combined standard uncertainty of the linewidth is calculated using Eq. (5).

3.4 Coverage factor

Since correlations exist between some of the input quantities of the measurement function, the effective degrees of freedom, ν_{eff}, of the combined standard uncertainty is calculated using the generalized Welch–Satterthwaite formula shown in Eq. (43), where r_{ij} denotes the correlation coefficient of x_i and x_j [8].

$$\nu_{\mathrm{eff}} = \frac{u_{\mathrm{c}}^4}{\sum_{i=1}^{n} \left(\sum_{j=1}^{n} c_i c_j u(x_i) u(x_j) r_{ij} \right)^2 / \nu_i} \tag{43}$$

Based on the effective degrees of freedom, the t-value corresponding to a 95 % coverage probability is obtained from the t-distribution table and used as the coverage factor.

$$k = t_{95\,\%, \nu_{\mathrm{eff}}} \tag{44}$$

3.5 Expanded uncertainty

Expanded uncertainty of the linewidth for a coverage probability of 95 % is obtained by multiplying the combined standard uncertainty with the coverage factor *k*.

$$U = k \cdot u_c \tag{45}$$

3.6 Worked example of an uncertainty budget

Table *1* presents an uncertainty budget illustrating the actual evaluation of measurement uncertainty for a line with a nominal width of 40 μm, using a 10× objective lens. The expanded uncertainty $(k = 2)$ is evaluated as 0.11 μm.

4. DISCUSSION

Through the thorough evaluation of measurement uncertainty according to the ISO/IEC 98-3, it was confirmed that although the measurement results attain metrological traceability through both the laser wavelength of the interferometer and the reference linewidth standard, the uncertainty contribution from the interferometer is negligible in comparison. The dominant source of overall measurement uncertainty arises from the reference linewidth standard used in calibrating the threshold ratio, which acts as a limiting factor.

The smallest available linewidth measurement uncertainty from calibration services of National Metrology Institutes (NMIs) is 20 nm (with a coverage factor of $k = 2$, corresponding to a level of confidence of approximately 95 %). If the linewidth standards are calibrated by such an NMI, the expanded uncertainty of the linewidth measured by the developed system could potentially be reduced to as low as 47 nm ($k = 2$).

5. CONCLUSION

An optical microscopic system for the precise calibration of linewidths was developed and calibrated using both a laser interferometer and a certified reference linewidth standard. This study presented the system configuration and outlined the detailed procedures employed for evaluating the measurement uncertainty associated with the linewidth measurements. At present, the expanded uncertainty of linewidth measurements obtained using the developed system is 0.11 μm ($k = 2$, corresponding to

approximately 95 % coverage probability). However, if the reference linewidth standards are calibrated by an NMI with a smaller uncertainty, the overall measurement uncertainty could potentially be reduced to as low as 47 nm

Table 1

Uncertainty budget for a 40 µm linewidth measurement, using the 10× objective lens.

Input quantity X_i	Estimate x_i	Standard uncertainty $u(x_i)$	Sensitivity coefficient c_i	Uncertainty contribution u_i	Probability distribution	Degrees of freedom v_i
L	320.475 7 µm	0.037 9 µm	0.124 8	0.004 7 µm	t	9
L_r	320.476 µm	0.037 6 µm	-	-	t	9
L_λ	0 µm	0.000 0 µm	-	-	Rectangular	∞
L_n	0 µm	0.000 7 µm	-	-	t	∞
L_c	0 µm	0.000 4 µm	-	-	Rectangular	50
L_{Ab}	0 µm	0.004 2 µm	-	-	Rectangular	50
L_{nl}	0 µm	0.000 6 µm	-	-	Rectangular	∞
ΔP	1906.142	0.219	0.021 0 µm	0.004 6 µm	t	9
ΔP_{ran}	0	0.035	-	-	Normal	∞
ΔP_{res}	0	0.217	-	-	t	9
T_c	0.370 10	0.025	-2.142 9 µm	0.053 4 µm	t	4.3×10^{8}
$I_{th,ref}$	86.065	5.79	0.004 3	0.024 9	t	∞
$I_{th,ref,cal}$	-	5.43	-	-	Normal	∞
$I_{th,ref,dev}$	-	2.01	-	-	Rectangular	∞
ΔI_{ref}	232.544	0.019	0.001 59	3.1×10^{-5}	t	1946
$I_{up,ref}$	232.54	0.019	-	-	t	1799
$I_{low,ref}$	0.00	0.004	-	-	t	655
δT_c	0.000 0	0.000 3	1	0.000 3	t	9
ΔI	232.54	0.019	-0.003 41 µm	0.000 1 µm	t	1946
a_1	35.169 4	0.590 9	-0.568 40 µm	0.335 9 µm	t	5
b_1	4267.70	70.208 8	0.004 78 µm	0.335 6 µm	t	5
a_2	-37.913 0	0.504 3	0.527 27 µm	0.265 9 µm	t	5
b_2	4593.92	59.930 0	0.004 43 µm	0.265 8µm	t	5
l_t	0 µm	1.3×10^{-5} µm	1	1.3×10^{-5} µm	Rectangular	∞
α	5.50×10^{-7} /°C	9.13×10^{-9} /°C	0 µm°C	0 µm	Rectangular	50
t	20 °C	0.59 °C	2.2×10^{-5} µm/°C	1.3×10^{-5} µm	Rectangular	∞
t_a	20 °C	0.58 °C	-	-	Rectangular	∞
δt	0 °C	0.12 °C	-	-	Rectangular	∞
δl_r	0 µm	0.000 8 µm	1	0.000 8 µm	t	9
δl_f	0 µm	0.007 8 µm	1	0.007 8 µm	Rectangular	50
δl_c	0 µm	3.5×10^{-5} µm	1	3.5×10^{-5} µm	Rectangular	50
$u(a_1,b_1)$	-	41.487 9	-0.005 43 µm^2	-0.225 5 µm^2	-	-
$u(a_2,b_2)$	-	-30.224 2	0.004 68 µm^2	-0.141 3 µm^2	-	-
W_L	**39.981 µm**	**0.054 µm**	-	**-**	t	**2 409**

6. ACKNOWLEDGEMENT

This work was supported by the KRISS under the project "Development of Innovative Technologies for Length and Angle Measurement Standards," GP2025-0001-05.

7. REFERENCES

[1] Cattin, P., Küng, J., Dürig, U., et al., Traceable linewidth measurements in the nanometre range by optical microscopy, Measurement Science and Technology, Volume 13, Issue 10, 2002, Pages: 1523–1530.

[2] Dai, G., Dixson, R. G., Postek, M. T., Critical dimension metrology with the scanning electron microscope: Modeling the lineshape measured by SEM, Journal of Vacuum Science and Technology B, Volume 24, Issue 1, 2006, Pages: 309–320.

[3] Dai, G., Postek, M. T., Dixson, R. G., Song, J. F., Vladár, A. E., Traceable linewidth metrology using critical dimension atomic force microscopes, Journal of Vacuum Science and Technology B, Volume 25, Issue 6, 2007, Pages: 2113–2121.

[4] Lee, J.Y., et. al., *An optical system for precise measurement of linewidth*, in preparation

[5] Kim, J.-A., Kim, J. W., Kang, C.-S., Eom, T. B., Ahn, J., *A digital signal processing module for real-time compensation of nonlinearity in a homodyne interferometer using a field-programmable gate array,* Measurement Science and Technology, Volume 20, Issue 1, 2009, Pages: 017003.

[6] ISO/IEC, ISO/IEC Guide 98-3:2008, *Uncertainty of measurement, Part 3: Guide to the expression of uncertainty in measurement,* 2008.

[7] Bönsch, G., Potulski, E., *Measurement of the refractive index of air and comparison with modified Edlén's formulae*, Metrologia, Volume 35, Issue 2, 1998, Pages: 133.

[8] Willink, R., *A generalization of the Welch–Satterthwaite formula for use with correlated uncertainty components*, Metrologia, Volume 44, Issue 5, 2007, Pages: 340.

Evaluarea incertitudinii în măsurarea lățimii liniilor utilizând un sistem optic microscopic calibrat atât cu un interferometru laser, cât și cu un etalon de lățime de linie

A fost dezvoltat un sistem optic microscopic pentru măsurarea precisă a lățimii liniilor. Sistemul este capabil să măsoare lățimi de linie care sunt fie mai înguste, fie mai largi decât câmpul vizual al microscopului și poate fi aplicat atât liniilor transparente, cât și celor opace. Sistemul este calibrat folosind un interferometru laser și un etalon de lățime de linie, acesta din urmă fiind calibrat de un Institut Național de Metrologie străin. Această lucrare prezintă sistemul de măsurare și oferă o evaluare detaliată a incertitudinii de măsurare.

Chu-Shik KANG, Ph.D., Principal Research Scientist, Korea Research Institute of Standards and Science, Length & Dimensional Metrology Group; Professor, University of Science and Technology, Precision Measurement, cskang@kriss.re.kr, +82 42 868 5103, 267 Gajeong-ro, Yuseong-gu, Daejeon, 34113, Republic of Korea

Jae Yong Lee, Ph.D., Principal Research Scientist, Korea Research Institute of Standards and Science, Length & Dimensional Metrology Group, jaeyong@kriss.re.kr, +82 42 868 5226, 267 Gajeong-ro, Yuseong-gu, Daejeon, 34113, Republic of Korea

Sunghoon EOM, M.S., Senior Engineer, Korea Research Institute of Standards and Science, Length & Dimensional Metrology Group, sheom@kriss.re.kr, +82 42 868 5100, 267 Gajeong-ro, Yuseong-gu, Daejeon, 34113, Republic of Korea

Jong-Ahn KIM, Ph.D., Principal Research Scientist, Korea Research Institute of Standards and Science, Length & Dimensional Metrology Group, jakim@kriss.re.kr, +82 42 868 5683, 267 Gajeong-ro, Yuseong-gu, Daejeon, 34113, Republic of Korea

Jae Heun WOO, Ph.D., Senior Research Scientist, Korea Research Institute of Standards and Science, Length & Dimensional Metrology Group, jhwoo@kriss.re.kr, +82 42 868 5668, 267 Gajeong-ro, Yuseong-gu, Daejeon, 34113, Republic of Korea